JOURNAL OF MATERIALS SCIENCE 37 (2002) 2483–2490

Microstructure, texture, and mechanical properties of continuously cast gamma TiAl

M. L. WEAVER, C. W. CALHOUN
Department of Metallurgical and Materials Engineering, University of Alabama, Tuscaloosa, AL 35487-0202, USA
E-mail: mweaver@coe.eng.ua.edu

H. GARMESTANI
Department of Mechanical Engineering, FAMU-FSU College of Engineering, Tallahassee, FL 32310-2175, USA

Microstructural and texture analyses have been conducted on two gamma titanium aluminide (γ-TiAl) sheets produced via the melt overflow rapid solidification technique. For both alloy compositions relatively weak $\{101\}_\gamma$ type fiber textures ($\leq 3\times$ random) were observed which are indicative of solidification from a prior α phase field with rapid growth parallel to the $[10\bar{1}0]_\alpha$ direction. The strengths of the strips were comparable to conventionally processed sheets however tensile ductility was low. The results are discussed with respect to recent studies of the influence of cooling rate on the solidification microstructure of cast titanium aluminides.

1. Introduction

Gamma titanium aluminides are viable candidates for use in advanced high-temperature structural applications. Their favorable combinations of low density, high elastic modulus, good high-temperature strength retention, and good oxidation resistance allow them to exceed the operating temperatures of advanced titanium alloys and nickel- or iron-based superalloys up to 1073 K [1]. As a result, cast γ-based alloys are being considered for advanced automotive and aerospace applications. However, widespread use of γ-based alloys has been slowed to some extent by poor formability and high yield losses during thermomechanical processing leading to higher fabrication costs. Within the last decade, several research efforts have been directed towards the development of more cost effective processing techniques and understanding the relationships between processing technique, microstructure and mechanical behavior [2–11]. In one such effort, Gaspar *et al.* [12–15] have reported success in direct casting of strips of conventional titanium alloys and ordered intermetallic alloys using a single-chill-roll rapid solidification casting technique. Known as the Melt Overflow Rapid Solidification Technique (MORST), this method offers a net shape capability for the production of thin strips or foils with lower associated yield losses and improved chemical and microstructural homogeneity than traditional ingot metallurgy techniques. MORST has been successfully used to produce 0.5 mm thick × 10 cm wide × 3000–4000 mm long strips of orthorhombic, α_2-based, and γ-based intermetallic alloys, which are suitable for cold or hot rolling to foil gage (~0.1 mm thickness) with minimal waste. Like other methods of fabrication, processing via MORST can result in pronounced crystallographic textures, which can greatly influence the resulting properties of the material [16]. This paper summarizes the results of an investigation of the microstructures, textures, and room-temperature mechanical properties observed in MORST processed γ-TiAl strips.

2. Experimental

Two γ-TiAl strips were cast in the plasma melt overflow furnace at Ribbon Technology Corporation, Columbus, Ohio. This furnace combines plasma arc melting in a cold copper hearth which is rotated about the same axis of rotation as the chill roll to overflow liquid onto the circumference of a molybdenum chill roll [12, 13, 15]. All melting and casting was conducted in an atmosphere of purified argon. Two different chill roll surfaces were used: one with a 60°, 25-pitch diamond knurl pattern (Strip 1); the other with a mechanically peened surface (Strip 2). The as-cast thickness of strips 1 and 2 were 510 μm and 680 μm respectively. Post-processing chemical analyses were conducted using energy dispersive spectroscopy (EDS) for Ti, Al, Nb, and Cr, inert gas fusion for O and N, and combustion techniques for C. The results of these analyses are indicated in Table I.

Portions of the alloy strip were cut using a low speed diamond saw, mounted in Bakelite and polished to a 0.05 μm finish. Light optical microscopy (LOM) and scanning electron microscopy specimens were examined in both the etched and unetched conditions. Scanning electron microscopy examinations were conducted on a Philips XL 30 scanning electron microscope (SEM) operated at 20 kV. A solution consisting of 10 ml hydrofluoric acid, 5 ml nitric acid, 35 ml hydrogen peroxide, and 100 ml water was used for etching.

TABLE I Chemical composition of TiAl alloy

Strip # substrate	Element	Ti	Al	Nb	Cr	C	O	N
1	at.%	46.1	49.4	2.1	2.2	0.03	0.15	0.02
Knurled	wt%	57.3	34.6	5.0	3.0	0.01	0.06	0.01
2	at.%	48.2	47.2	2.1	2.1	0.03	0.16	0.03
Peened	wt%	59.3	32.7	5.1	2.8	0.01	0.06	0.01

Ti, Al, Nb, and Cr contents determined using energy dispersive spectroscopy.
O and N contents determined using inert gas fusion.
C content determined using combustion.

Texture variations in the γ and α_2 phases were measured using the x-ray diffraction (XRD) technique on a Philips X'Pert PW 3040 MRD x-ray diffractometer operating at 40 kV and 45 mA. The following incomplete pole figures were measured using Ni filtered Cu K_α radiation to determine texture: {100), {111}, {200) + {002), {220) + {202), $\{0002\}_{\alpha 2}$, $\{20\bar{2}0\}_{\alpha 2}$, $\{20\bar{2}1\}$, and $\{22\bar{4}0\}$. To account for the tetragonality of the γ phase, the crystallographic planes and directions have been expressed according to the rule proposed by Hug *et al.* [17]. The pole figure data was analyzed using the popLA software package [18]. Due to the tetragonality of the γ unit cell, the <100] and [001] reflections are non-equivalent and their peak locations in the 2θ scans overlap. Similarly, the <110] and <101] reflections also overlap. To separate the overlapping peaks, the Sample Orientation Distribution (SOD) was computed from a set of measured incomplete pole figures using the WIMV algorithm. Recalculations of the complete pole figures for each overlapping reflection and calculations of the inverse pole figures were then obtained from the SOD.

Mechanical properties were evaluated using a combination of Vickers microhardness and uniaxial tensile tests. Vickers microhardness measurements were conducted on transverse sections, through the thickness of each strip. Dogbone tensile specimens with gage lengths of 13.5 mm were cut from the cast strips such that the tensile axes were parallel to the casting direction. Mechanical tests were performed on a screw driven load frame at constant crosshead velocities corresponding to an initial strain rate of 2.8×10^{-5} s^{-1}. True stress-strain data were determined from the resulting load-time plots.

3. Results

Within experimental accuracy, the major differences between the two materials are the Ti and Al contents. Strip 1 contained 49.4 at.% Al while strip 2 contained 47.2 at.%Al. The differences in composition have been traced to the feedstock used in the casting process. The interstitial levels for both strips are equivalent and compare favorably with conventionally processed materials [19, 20].

Photomicrographs of the free and chill cast surfaces are provided in Fig. 1. For both strips, the substrate cast surfaces of each strip replicated the pattern on the

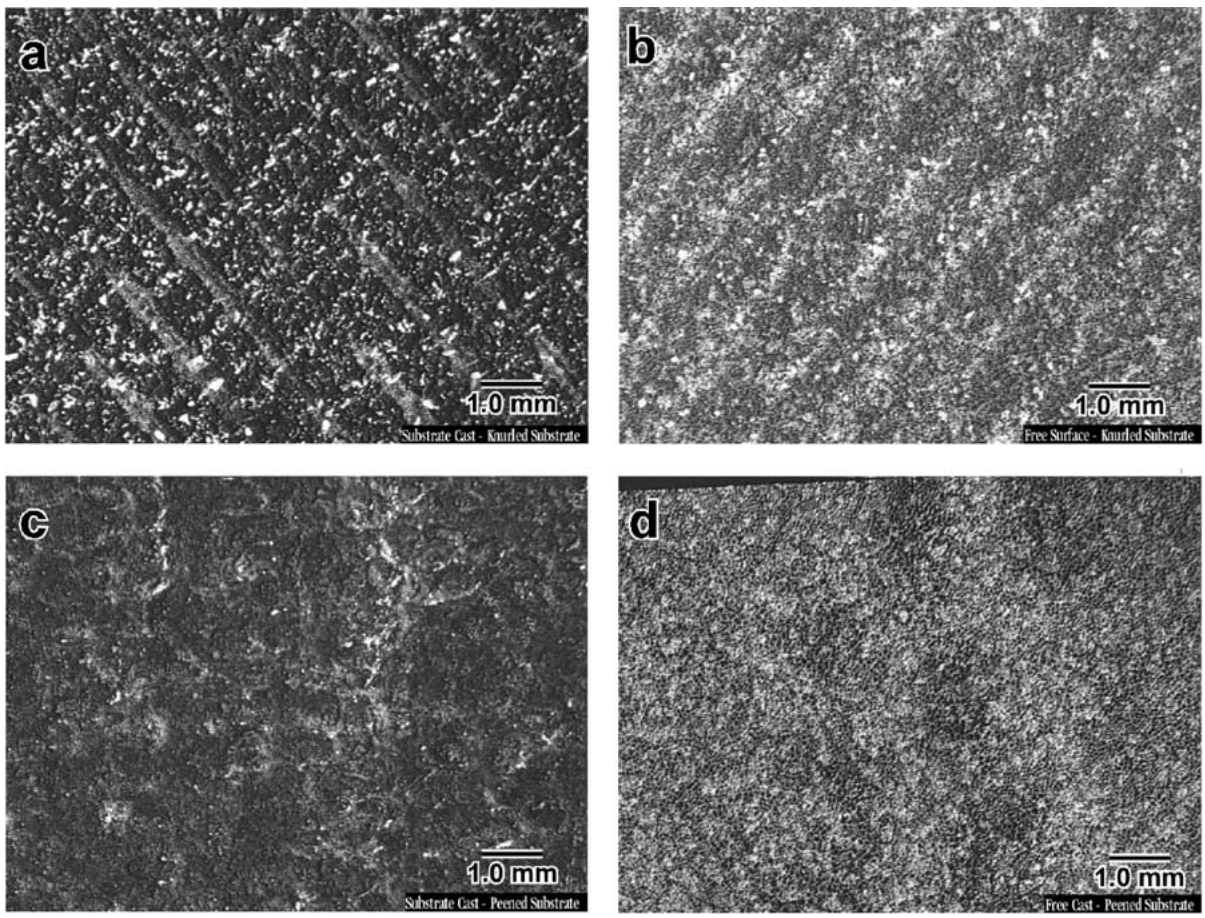

Figure 1 Surface morphologies of as-cast γ-TiAl strips; (a) substrate-cast surface of strip 1; (b) free-cast surface of strip 1; (c) substrate-cast surface of strip 2; and (d) free-cast surface of strip 2.

chill roll surface. For example, the substrate cast surface of strip 1, which was cast on the knurled chill roll surface, exhibited a clearly visible crosshatched pattern (Fig. 1a). This pattern was observed to extend through to the free cast surface of the strip (Fig. 1b), which is noticeably smoother than the substrate cast surface. Similarly, the substrate cast surface of strip 2 exhibited a somewhat pebbled appearance (Fig. 1c), representative of the peened chill roll while the free cast surface (Fig. 1d) was generally wavy and devoid of the pebbled pattern on the chill roll. Surface roughness was not evaluated in this investigation, however, it can be generally stated that the surfaces of strip 2 were smoother than those of strip 1. This statement is substantiated by the results of surface profilometry studies performed by Gaspar *et al.* [15] on strip 1 and Das [21] on strip 2. They reported average rms roughness values of $\sim$35 μm and 26 μm for the substrate and free cast sides respectively of strip 1 and $\sim$1.7 μm and $\sim$2.5 μm respectively for the substrate and free cast sides of strip 2.

Beyond the appearance of crosshatched, pebbled, or wavy patterns on the strip surfaces, both strips displayed a shiny metallic sheen on the substrate cast side and dull gray on the free cast side. Closer examinations of the free surface morphologies of the as-cast strips are presented in Fig. 2. The surfaces of both strips consisted of collections of dendrites, which were predominantly arranged in the form of equiaxed rosettes. The individual rosette arms were generally rotated by 60° with respect to each other as indicated by the arrows in Fig. 2b and d. Some regions on both strips exhibited no distinct crystallographic symmetry. Valencia *et al.* [22, 23] and McCullough *et al.* [24] reported similar dendrite morphologies in rapidly solidified γ-TiAl powders and in supercooled droplets, from which they tentatively identified the primary phase of solidification to be hexagonal α [22–25]. Similar dendrite morphologies were observed on the chill surfaces without the apparent solidification shrinkage between rosettes.

The longitudinal microstructures for the two TiAl strips are presented in Figs 3 and 4. Strip 1 (Fig. 3a) exhibited a microstructure consisting of readily apparent columns that often extended through its thickness. The columns tended to lean towards the leading edge of the strip (i.e., towards the casting direction) at an angle of approximately 10 degrees from the strip normal. Each column was observed to be composed of a series of grains, all of which consisted of a mixture of α_2 and γ lamellae (Fig. 3b and c). The grains themselves were almost always smaller and more equiaxed near the wheel contact (i.e., substrate) side of the strip, and larger and more elongated near the free side of the strip. The lamellar orientations within each grain ranged from approximately parallel to the wheel contact surface (i.e., perpendicular to the columnar growth direction) to a near 90° inclination. Similar observations have been reported for other rapidly solidified γ-based alloys [21, 26–28]. The slightly inclined columnar features can be attributed to the flow of undercooled melt ahead of the growing crystals [29].

The microstructure observed in strip 2 (Fig. 4a) was devoid of the columnar features observed in strip 1. The microstructure was composed of a heterogeneous mixture of relatively fine equiaxed grains and acicular features which appeared to transition to a more cellular appearance near the center of the strip. Coarse, somewhat

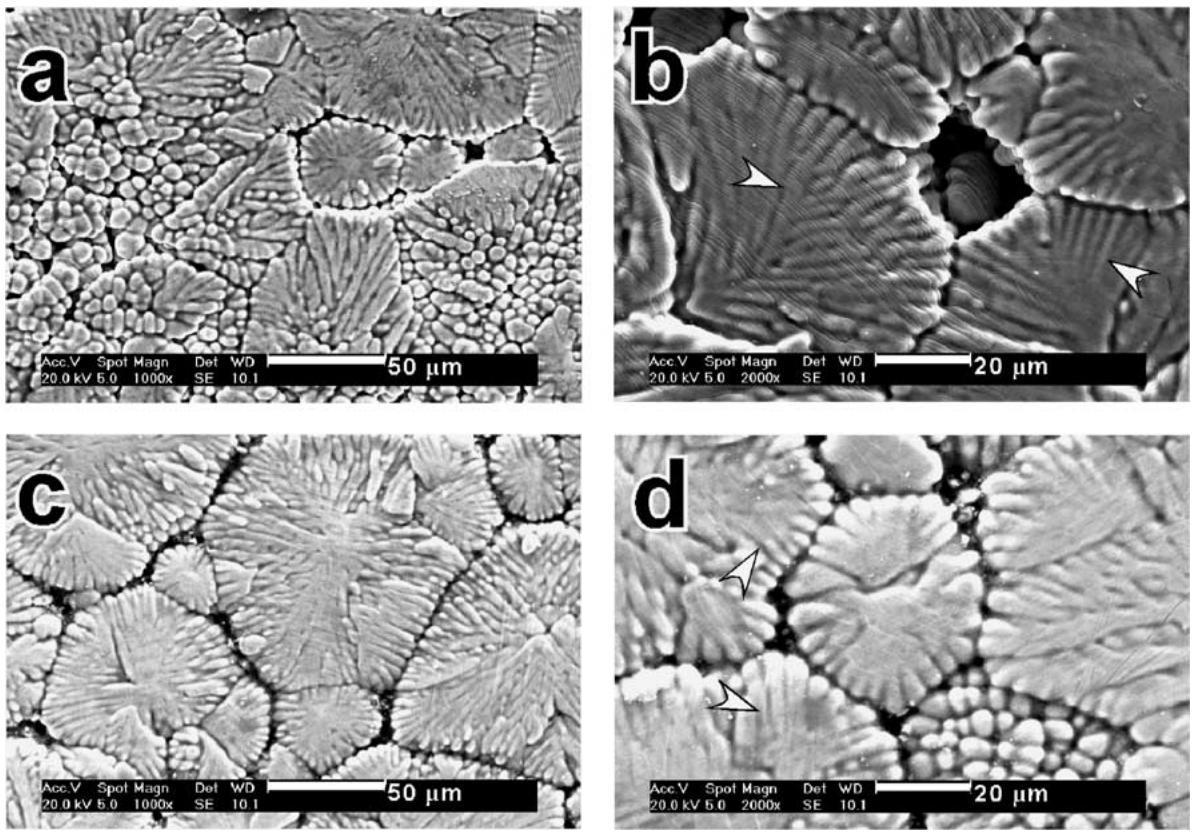

Figure 2 Free surface morphologies of as-cast γ-TiAl strips; (a, b) strip 1 and (c, d) strip 2.

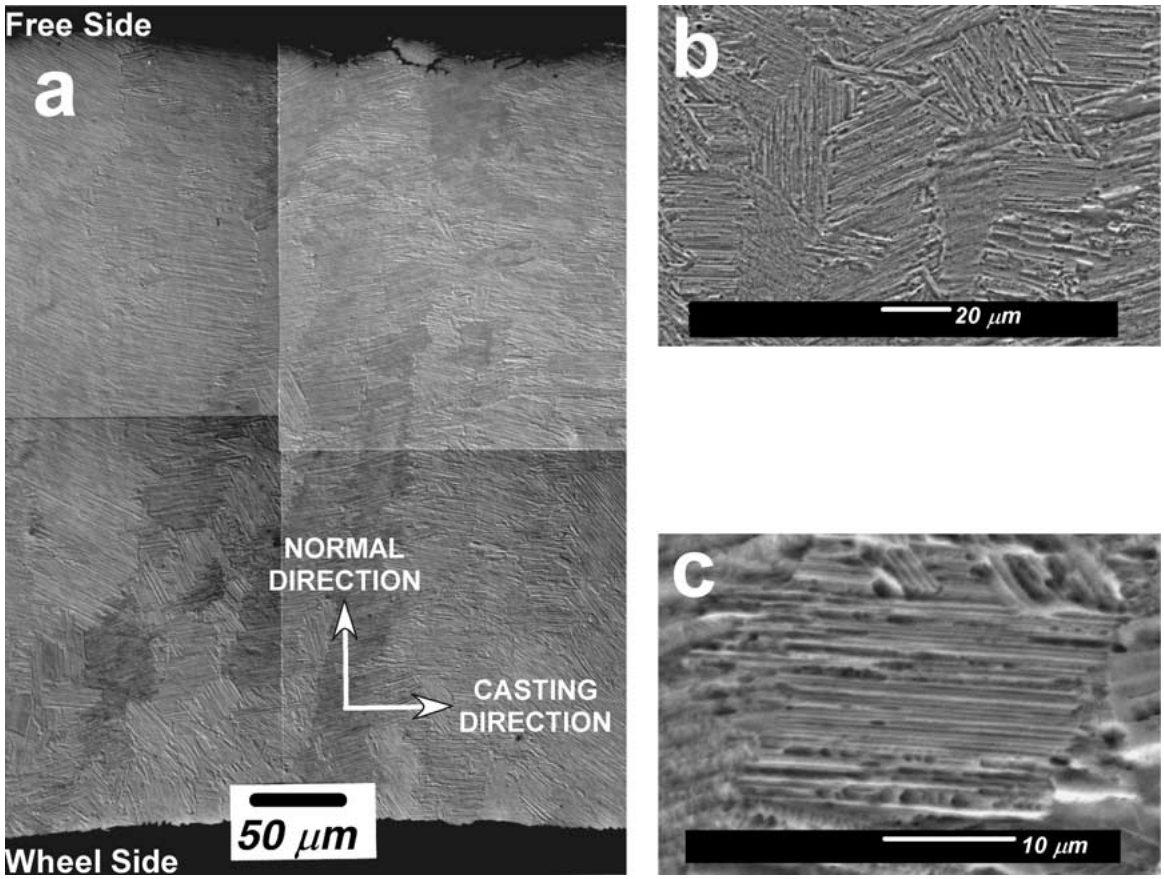

Figure 3 Microstructure of γ-TiAl strip 1; (a) through thickness morphology; (b and c) close-up of fine lamellar regions.

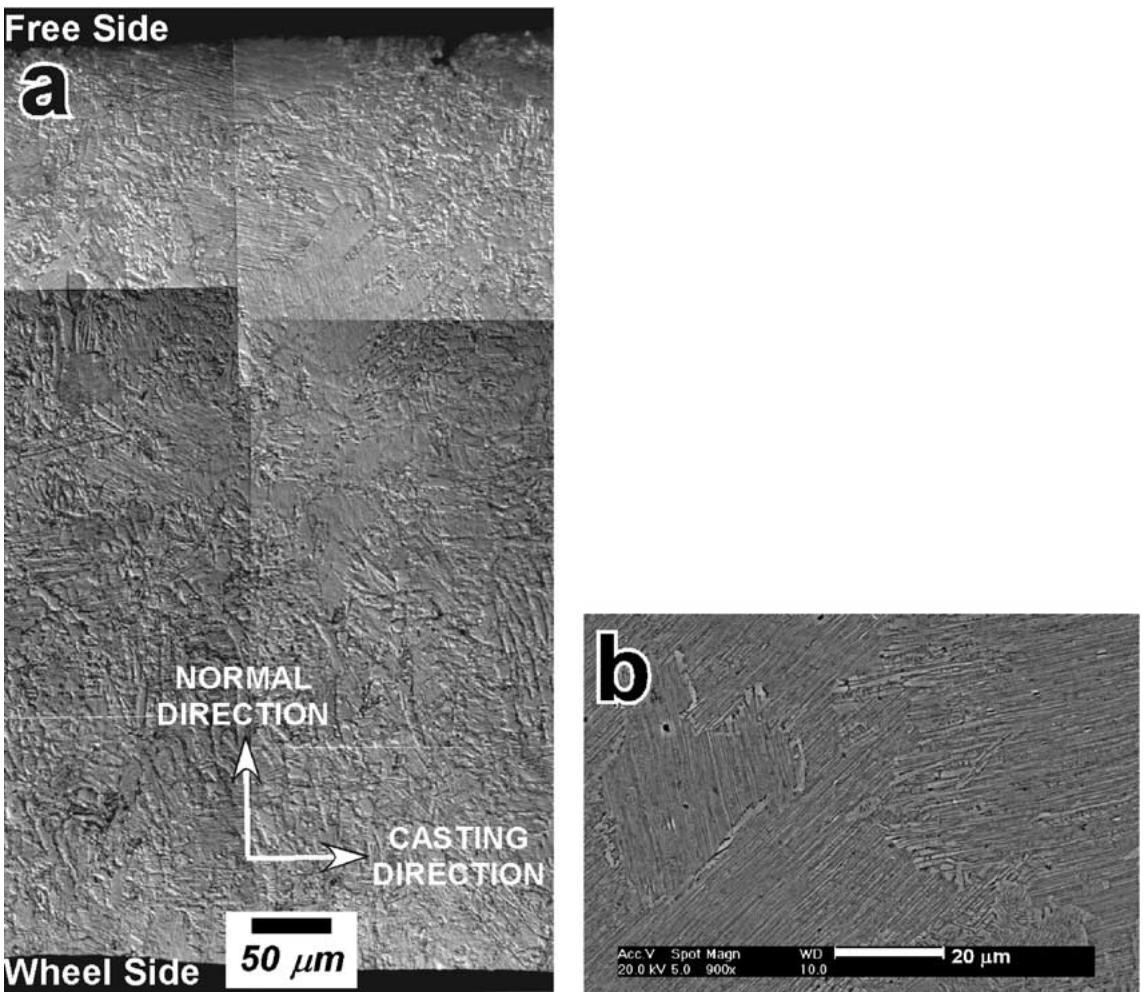

Figure 4 Microstructure of γ-TiAl strip 2; (a) through thickness morphology; (b) close-up of fine lamellar regions.

equiaxed features were observed near the free surface of the strip. The individual grains of strip 2 transformed during cooling to a mixture of fine lamellar $\alpha_2 + \gamma$ and patches of feathery γ (Fig. 4b). Consistent with the observations of Gaspar *et al.* [15] and Das [21], small amounts of porosity were present near the free surfaces of both strips. This porosity is likely the result of trapped gas and solidification shrinkage.

Through thickness texture variations observed in strip 2 are presented in Figs 5 and 6. In all, four specimens taken from random regions of the cast strip were analyzed. In all specimens, weak $\{101\}_\gamma$ type fiber textures ($\leq 3\times$ random), were observed through the thickness of the strip (Fig. 5). Recalculated pole figures for the α_2-phase are presented in Fig. 6. Weak $\{0002\}_{\alpha 2}$, $\{10\bar{1}0\}_{\alpha 2}$, and $\{11\bar{2}0\}_{\alpha 2}$ fiber textures, all with intensities ranging from ~ 2 to $\sim 3\times$ random, were observed as illustrated in the pole figures in Fig. 6.

The mechanical properties for both strips are summarized in Fig. 7 and in Table II. In both strips, microhardness remained relatively constant through the strip thickness, which can be taken qualitatively to indicate a relative lack of any significant chemical segregation. This was later confirmed via through thickness EDS analysis of the cast strips. The average microhardness values for both strips were essentially the same ($\sim$325 kg/mm^2). The measured tensile or fracture strengths were consistently higher in strip 2 than in strip 1 (Table II). All of the tensile specimens exhibited less than one-percent plastic elongation prior to failure. Analysis of the fracture surfaces showed that fracture occurred via a mixture of inter- and trans-lamellar cleavage (Fig. 8a). In all specimens fracture initiated at casting induced micropores near the specimen surfaces (Fig. 8b).

TABLE II Results of room-temperature tensile tests for various samples

Sample	Strip	Condition	Hardness (kg/mm^2)	σ_f (MPa)	$\sigma_{0.2}$ (MPa)	ε_{pl} (%)
A	1	As-cast		395	325	0.4
B	1	As-cast	331 ± 27	340	250	0.7
C	1	As-cast		382	372	0.6
E	2	As-cast		427[a]	–	–
F	2	As-cast	325 ± 25	487[a]	–	–
G	2	As-cast		445	445	0.2

[a]Failed at surface flaw.

4. Discussion

In this investigation, the microstructures and mechanical properties of two rapidly solidified γ-TiAl alloys have been studied. Based on the chemical compositions of the strips and the equilibrium phase diagram, it

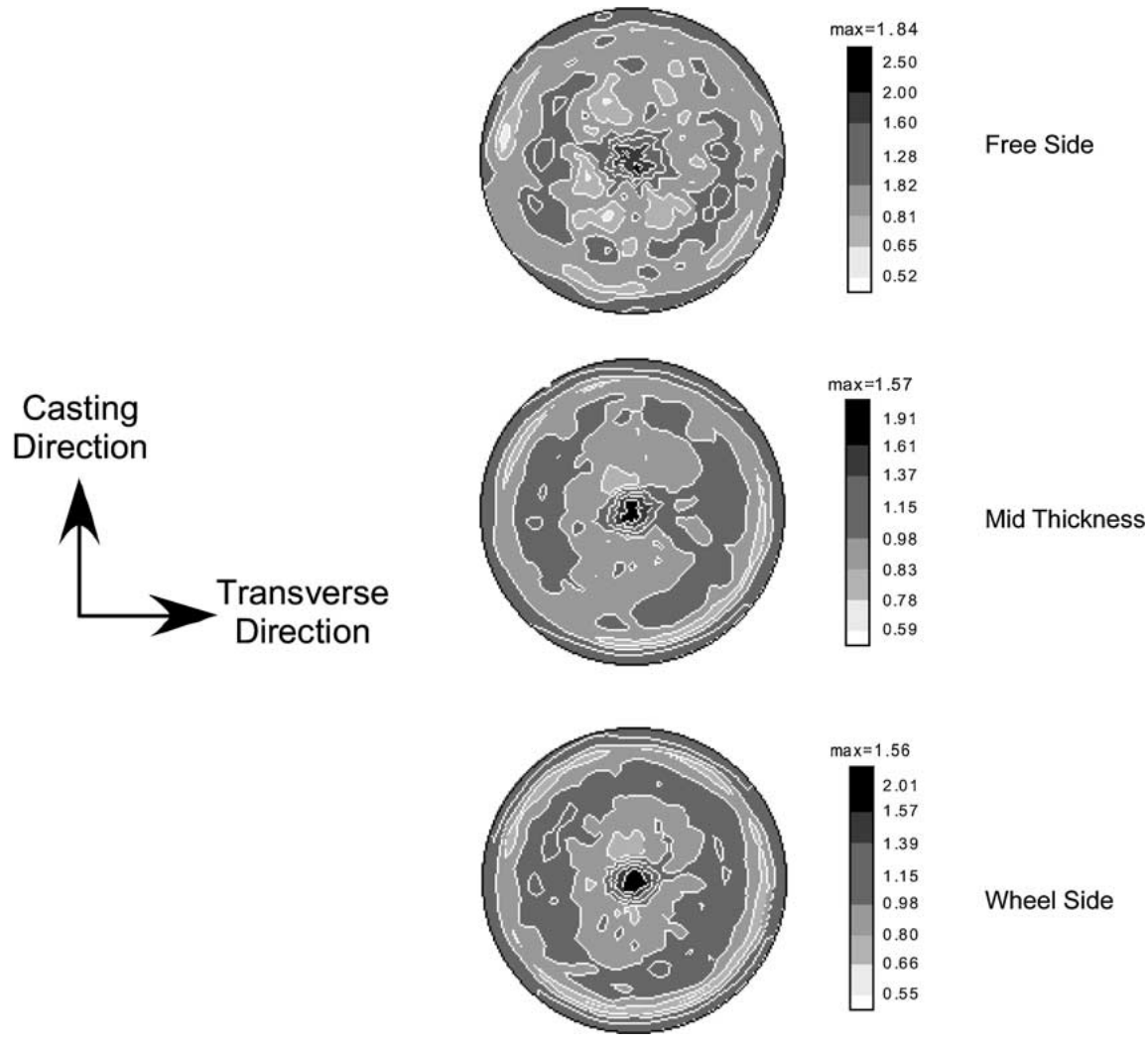

Figure 5 Representative $\{101\}_\gamma$ pole figures for the γ phase in strip 2. Similar textures were observed in strip 1.

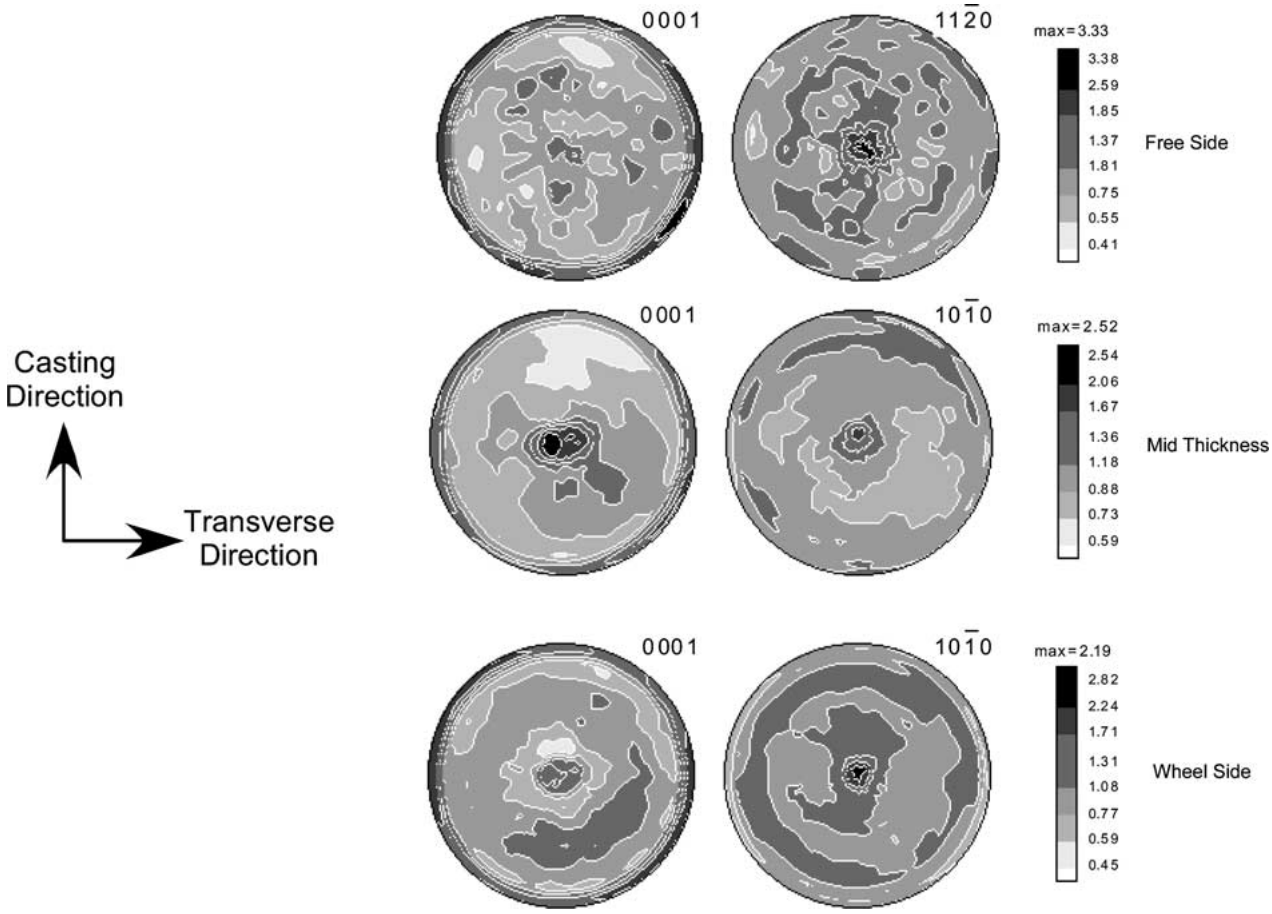

Figure 6 Representative pole figures for the α_2-phase in strip 2. Similar textures were observed in strip 1.

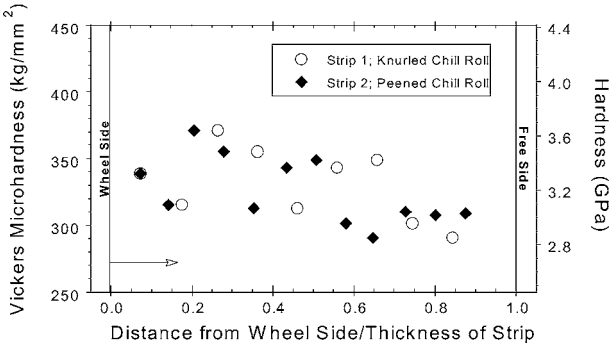

Figure 7 Through thickness microhardness variations for TiAl strips 1 and 2.

was expected that each would solidify from a primary β (bcc) phase field, which should yield strong $\{100\}_\gamma$ textures in the as-cast strips [30]. The presence of $\{101\}_\gamma$ fiber textures in this study instead suggests that the primary phase of solidification is α (hcp), an observation that is partially supported by the observance of hexagonal dendrite symmetry on the surfaces of the cast strips (see Fig. 2). As noted by DeGraef *et al.* [30], when γ alloys solidify from a primary α phase, the resulting γ textures will depend on the primary direction of solidification for the α phase. In conventional hexagonal close packed metals, the primary direction of solidification is usually $[10\bar{1}0]$ rather than [0001]. This is because the close packed planes in HCP systems will grow more rapidly laterally than along the normal. When primary solidification from α occurs in the $[10\bar{1}0]_\alpha$ direction (i.e., laterally in the basal plane), $\{101\}_\gamma$ or $\{110\}_\gamma$ type textures will result. Whereas, when the primary direction of solidification is $[0001]_\alpha$, a $\{111\}_\gamma$ texture will result. In several studies of rapidly solidified TiAl alloys, $\{111\}_\gamma$ textures have been reported [2, 3, 25, 26, 31, 32]. It has been suggested, however, that such textures will only persist for rapid dendrite tip velocities [30] where primary solidification might occur more preferentially along the $[0001]_\alpha$ direction. The $\{101\}_\gamma$ textures observed in the present study are in agreement with the observations of DeGraef who noted that for slowly cooled Ti-48at.%-2at.%Nb-2at.%Cr, that $\{101\}_\gamma$ textures occurred consistent with more rapid α growth along the $[10\bar{1}0]$ direction.

The cast microstructures for both strips were noticeably different; strip 1 consisting of a transformed columnar microstructure and strip 2 consisting of a more random mixture of fine equiaxed and acicular features. The structural differences likely result from slight differences in composition and cooling rate for the respective strips. Clearly, for strips of the same composition, a lower cooling rate could yield larger grains and fully lamellar structures as was recently shown by DeGraef *et al.* [30] who studied the influence of cooling rate on the microstructures of TiAl plates. Similarly, compositional differences could suppress grain growth and retard the phase transformation kinetics resulting in more coarse structures.

Numerous studies have been conducted to determine the influence of microstructural and compositional variations on the mechanical properties of γ-TiAl alloys

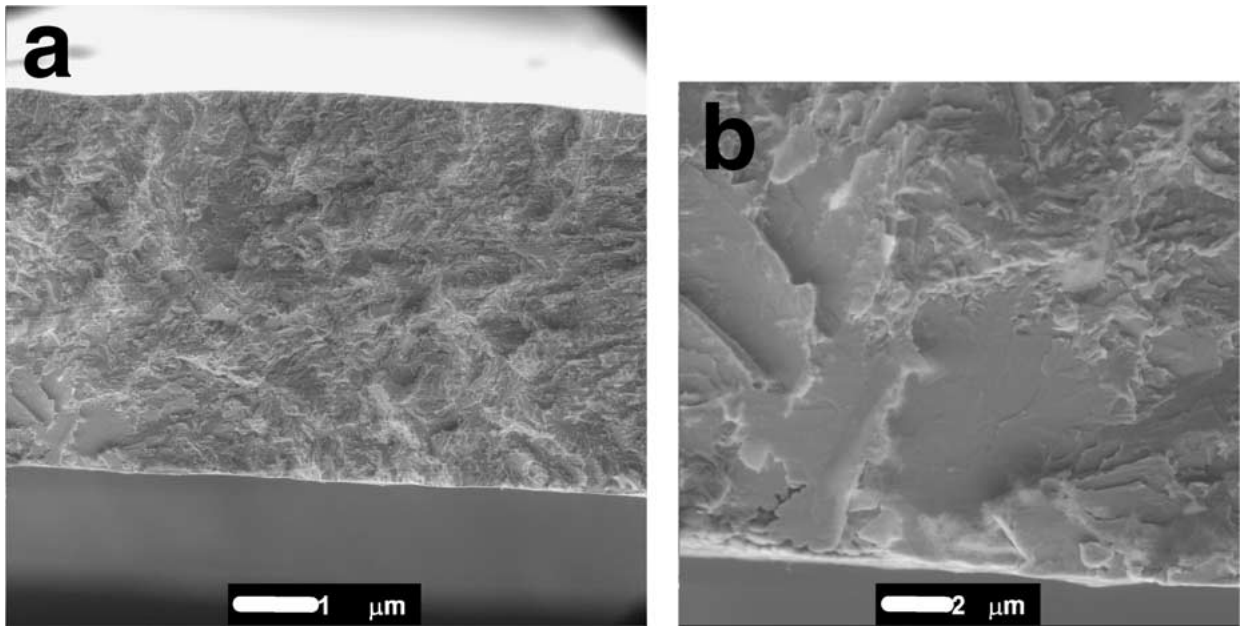

Figure 8 Representative fracture surface of a cast γ-TiAl sheet deformed at room temperature; (a) general fracture surface and (b) close-up of fracture initiation site.

(see for example references [33–36]). In general, it has been shown that differences in composition and microstructural variables, in particular grain/colony size, can yield significant differences in mechanical properties. In the present investigation, both strips exhibited essentially the same Vickers microhardness as measured through the strip thickness. The tensile strengths measured parallel to the casting direction were equivalent to some wrought γ-TiAl products [4, 37], but were different for each strip. Strip 2 was found to exhibit a higher tensile strength and a lower tensile ductility than strip 1. Tensile ductility in both strips was extremely low (less than one percent ductility) compared to wrought γ-TiAl products, which typically exhibit two to five percent ductility [4, 37]. The differences in strength and ductility can be partially explained in terms of the slight differences in composition between the two strips. Strip 1, for example, contains 49.4 at.% Al compared with strip 2, which contains 47.2 at.% Al. Kobayashi *et al.* [38], who recently investigated the influence of stoichiometry on the properties of binary and ternary TiAl alloys showed that the 0.2% compressive flow stress of ternary TiAl-4 at.%Cr alloys decreased with increasing Al content. Our observations are consistent in that strip 2, which contains lower concentrations of Al, is stronger than strip 1.

The differences in properties between the two strips can also be explained in terms of the microstructures in each of the cast strips. From Figs 3 and 4 it is clear that both strips exhibit significantly different microstructures. Strip 1 consists of a mixture of elongated and equiaxed lamellar colonies (Fig. 3) while strip 2 consists of a mixture of equiaxed lamellar colonies, acicular grains and cellular regions. In a series of recent investigations Koeppe *et al.* [4, 19] and Clemens *et al.* [37] noted that the ductility of TiAl alloys with equiaxed or duplex microstructures is governed by the homogeneity of grain size but is nearly independently of compositional effects. In other words, more homogeneous grain size distributions yield materials exhibiting higher ductility [19]. They also noted that strength is controlled more by the absolute value of grain size in addition to composition. In accord with the Hall-Petch relationship, materials with smaller grain sizes were stronger. Thus, it is likely that the low ductility observed in strips 1 and 2 compared to conventionally process materials is due in part to microstructural inhomogeneities, most notably wide variations in grain size, and variations in defect (i.e., porosity) content. Variations in surface roughness could also be a potential contributor towards the observed differences, though no definitive conclusions can be drawn from the present investigation.

Fracture, which occurred via a mixture of inter- and trans-lamellar cleavage, initiated at casting induced micropores near the specimen surfaces. It is anticipated that modest improvements in tensile ductility and strength can be obtained by removal of sub-surface casting porosity either via light rolling or grinding. Further investigations are in progress, however, it is noted that materials subjected to such treatments, however, will still exhibit inhomogeneous microstructures consisting of a wide range of grain sizes, which will still limit the ductility of the strips [19, 39].

5. Conclusions

The melt overflow rapid solidification technique was used to produce thin γ-TiAl strips. The microstructures of the strips consisted of a mixture of a mixture of feathery γ and lamellar $\alpha_2 + \gamma$ colonies. Relatively weak $<101]$ transformation textures were observed in the γ-phase which are consistent with solidification from a primary α phase. Tensile strengths of the cast strips are equivalent to some wrought γ-TiAl sheet materials; however, tensile ductility parallel to the rolling direction remains low. It is anticipated that modest improvements in tensile ductility can be obtained by removing of sub-surface casting porosity. Further improvements

will require the processing scheme to be modified to allow the production of materials with more homogeneous grain size distributions.

Acknowledgments

This research was supported by the NASA-Langley Research Center (LaRC) under the Faculty Awards for Research Program and School of Mines and Energy Development (SOMED) at The University of Alabama. The authors would like to thank Dr. G. Das, Pratt & Whitney and Mr. W. D. Brewer, NASA-LaRC, for supplying the cast strips and for helpful discussions.

References

1. Y. W. KIM, *JOM* **46** (1994) 30.
2. M. MATSUO, T. HANAMURA, M. KIMURA, N. MASAHASHI and T. TOSHIAKI, "Microstructure/Property Relationships in Titanium Aluminides and Alloys," edited by Y. W. Kim and R. R. Boyer (The Minerals, Metals & Materials Society, Warrendale, PA, 1991) p. 323.
3. M. MATSUO, T. HANAMURA, M. KIMURA, N. MASAHASHI, T. MIZOGUCHI and K. MIYAZAWA, *ISIJ International* **31** (1991) 289.
4. C. KOEPPE, A. BARTELS, H. CLEMENS, P. SCHRETTER and W. GLATZ, *Materials Science and Engineering A* **201** (1995) 182.
5. C. HARTIG, H. FUKUTOMI, H. MECKING and K. AOKI, *ISIJ International* **33** (1993) 313.
6. H. INOUE, Y. YOSHIDA and N. INAKAZU, *Journal of Japan Institute of Light Metals* **44** (1994) 646.
7. *Idem.*, *Materials Science Forum* **157–162** (1994) 721.
8. H. FUKUTOMI, S. TAKAGI, K. AOKI, M. NOBUKI, H. MECKING and T. KAMIJO, *Scripta Metallurgica et Materialia* **25** (1991) 1681.
9. H. FUKUTOMI, A. NOMOTO and T. OTA, *Materials Transactions, JIM* **35** (1995) 610.
10. H. FUKUTOMI, A. NOMOTO, Y. OSUGA, S. IKEDA and H. MECKING, *Intermetallics* **4** (1996) S49.
11. H. MECKING, J. SEEGER, C. HARTIG and G. FROMMEYER, *Materials Science Forum* **157–162** (1994) 813.
12. T. A. GASPAR and L. E. HACKMAN, *Materials Science and Engineering* A **133** (1991) 676.
13. T. A. GASPAR, L. E. HACKMAN, E. BATAWI and J. A. PETERS, *ibid.* A **170/180** (1994) 645.
14. T. A. GASPAR, I. M. SUKONNIK, R. K. BIRD and W. D. BREWER, "Synthesis/Processing of Lightweight Metallic Materials," edited by F. H. Froes, C. Suryanarayana and C. M. Ward-Close (The Minerals, Metals & Materials Society, Las Vegas, NV, 1995) p. 119.
15. T. A. GASPAR, T. A. STUART, I. M. SUKONNIK, S. L. SEMIATIN, E. BATAWI, J. A. PETERS and H. L. FRASER, NASA CR-4742, Ribbon Technology Corporation, 1996.
16. A. BARTELS, C. HARTIG, S. WILLEMS and H. UHLENHUT, *Materials Science and Engineering* A **239/240** (1997) 14.
17. G. HUG, A. LOISEAU and P. VEYSSIERE, *Phil. Mag.* A **57** (1988) 499.
18. J. KALLEND, U. F. KOCKS, A. D. ROLLETT and H.-R. WENK, *Materials Science and Engineering* A **132** (1991) 1.
19. C. KOEPPE, A. BARTELS, J. SEEGER and H. MECKING, *Metallurgical Transactions* A **24A** (1993) 1795.
20. P. L. MARTIN, S. K. JAIN and M. A. STUCKE, "Gamma Titanium Aluminides," edited by Y.-W. Kim, R. Wagner and M. Yamaguchi (The Minerals, Metals & Materials Society, Warrendale, PA, 1995) p. 727.
21. G. DAS, "Deformation and Fracture of Ordered Intermetallic Materials III," edited by W. O. Soboyejo, H. M. Fraser and T. F. Srivatsan (The Minerals, Metals & Materials Society, Warrendale, PA, 1996) p. 217.
22. J. J. VALENCIA, C. MCCULLOUGH, C. G. LEVI and R. MEHRABIAN, *Scripta Metallurgica* **21** (1987) 1341.
23. *Idem.*, *Acta Metallurgica* **37** (1989) 2517.
24. C. MCCULLOUGH, J. J. VALENCIA, C. G. LEVI and R. MEHRABIAN, *Materials Science and Engineering* A **124** (1990) 83.
25. *Idem.*, *Acta Metallurgica* **37** (1989) 1321.
26. E. L. HALL and S.-C. HUANG, *Acta Metallurgica et Materialia* **38** (1990) 539.
27. G. SHAO, T. GROSDIDIER and P. TSAKIROPOULOS, *Journal de Physique III* **3** (1993) 465.
28. *Idem.*, *ibid*. **3** (1993) 377.
29. H. WARLIMONT and K. EMMERICH, "Rapidly Cast Crystalline Thin Sheet Materials" (American Society for Metals, Metals Park, OH, 1986) p. 73.
30. M. DEGRAEF, N. BIERY, L. L. RISHEL, T. M. POLLOCK and A. W. CRAMB, "Gamma Titanium Aluminides 1999," edited by Y.-W. Kim, D. M. Dimiduk and M. H. Loretto (The Minerals, Metals & Materials Society, Warrendale, PA, 1999) p. 247.
31. D. VUJIC, Z. LI and S. H. WHANG, *Metallurgical Transactions* A **19A** (1988) 2445.
32. D. J. JOHNSON, H. INUI and M. YAMAGUCHI, *Intermetallics* **6** (1998) 647.
33. "Structural Intermetallics," edited by R. Darolia, J. J. Lewandowski, C. T. Liu, P. L. Martin, D. B. Miracle and M. V. Nathal (The Minerals, Metals & Materials Society, Warrendale, PA, 1993).
34. "Structural Intermetallics 1997," edited by M. V. Nathal, R. Darolia, C. T. Liu, P. L. Martin, D. B. Miracle, R. Wagner and M. Yamaguchi (The Minerals, Metals & Materials Society, Warrendale, PA, 1997).
35. "Gamma Titanium Aluminides," edited by Y.-W. Kim, R. Wagner and M. Yamaguchi (The Minerals, Metals & Materials Society, Warrendale, PA, 1995).
36. "Gamma Titanium Aluminides 1999," edited by Y.-W. Kim, D. M. Dimiduk and M. H. Loretto (The Minerals, Metals & Materials Society, Warrendale, PA, 1999).
37. H. CLEMENS, W. GLATZ, P. SCHRETTER, C. KOEPPE, A. BARTELS, R. BEHR and A. WANNER, "Gamma Titanium Aluminides," edited by Y.-W. Kim, R. Wagner and M. Yamaguchi (The Minerals, Metals & Materials Society, Warrendale, OH, 1995) p. 717.
38. E. KOBAYASHI, K. SHINMOTO, S. MIURA, T. SUZUKI and Y. MISHIMA, "Gamma Titanium Aluminides," edited by Y.-W. Kim, R. Wagner and M. Yamaguchi (The Minerals, Metals & Materials Society, Warrendale, PA, 1995) p. 347.
39. S.-C. HUANG and E. L. HALL, *Metallurgical Transactions* A **22A** (1991) 427.

Received 17 May 2001
and accepted 24 January 2002